This is an open access article published under a Creative Commons Attribution (CC-BY) License, which permits unrestricted use, distribution and reproduction in any medium, provided the author and source are cited.

ACS Biomaterials SCIENCE & ENGINEERING

Article

pubs.acs.org/journal/abseba

3D Printing PDMS Elastomer in a Hydrophilic Support Bath via Freeform Reversible Embedding

Thomas J. Hinton,[†] Andrew Hudson,[†] Kira Pusch,[‡] Andrew Lee,[†] and Adam W. Feinberg*[,†,‡]

[†]Department of Biomedical Engineering and [‡]Department of Materials Science and Engineering, Carnegie Mellon University, 5000 Forbes Avenue, Pittsburgh, Pennsylvania 15213 United States

Supporting Information

ABSTRACT: Polydimethylsiloxane (PDMS) elastomer is used in a wide range of biomaterial applications including microfluidics, cell culture substrates, flexible electronics, and medical devices. However, it has proved challenging to 3D print PDMS in complex structures due to its low elastic modulus and need for support during the printing process. Here we demonstrate the 3D printing of hydrophobic PDMS prepolymer resins within a hydrophilic Carbopol gel support via freeform reversible embedding (FRE). In the FRE printing process, the Carbopol support acts as a Bingham plastic that yields and fluidizes when the syringe tip of the 3D printer moves through it, but acts as a solid for the PDMS extruded within it. This, in combination with the immiscibility of hydrophobic PDMS in the hydrophilic Carbopol, confines the PDMS prepolymer within the support for curing times up to 72 h while maintaining dimensional stability. After printing and curing, the Carbopol support gel releases the embedded PDMS prints by using phosphate buffered saline solution to reduce the Carbopol yield stress. As proof-of-concept, we used Sylgard 184 PDMS to 3D print linear and helical filaments via continuous extrusion and cylindrical and helical tubes via layer-by-layer fabrication. Importantly, we show that the 3D printed tubes were manifold and perfusable. The results demonstrate that hydrophobic polymers with low viscosity and long cure times can be 3D printed using a hydrophilic support, expanding the range of biomaterials that can be used in additive manufacturing. Further, by implementing the technology using low cost open-source hardware and software tools, the FRE printing technique can be rapidly implemented for research applications.

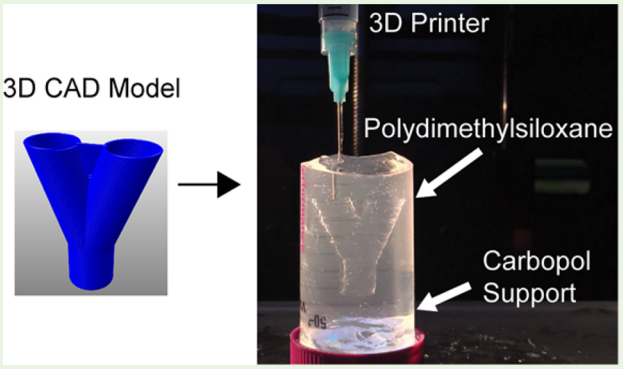

KEYWORDS: *3D printing, PDMS, FRE printing, freeform fabrication, Carbopol*

INTRODUCTION

Polydimethylsiloxane (PDMS) elastomer is a widely used biomaterial because of its biocompatibility,[1] optical transparency and low autofluorescence,[2] moldability with submicron resolution,[3] and high oxygen permeability.[4] The ease of fabrication by spin-coating or molding the liquid prepolymer and then cross-linking has led to a range of applications including microfluidics,[5,6] cell culture scaffolds,[7,8] flexible electronics,[9] and medical devices.[10] However, the low viscosity of the liquid prepolymer also makes it difficult to use PDMS in more advanced fabrication approaches, such as 3D printing. For thermoplastics, extrusion occurs at a melting temperature, and the material rapidly solidifies as it cools, requiring very little time for the fluid to transform into a solid. However, although a low viscosity for PDMS facilitates deposition from a syringe extruder, the relatively long gelation time results in flowing of the PDMS and loss of print fidelity. Further, PDMS has an elastic modulus of ~1 MPa or less, and thus requires a support material to print complex 3D structures. However, the hydrophobicity and low surface energy of PDMS limit the materials that can be effectively coprinted.

Advances in additive manufacturing and the maker movement have led to a number of improved methods for 3D printing using PDMS. For example, there are room temperature vulcanizing PDMS sealants with thixotropic flow properties that can be 3D printed in air and have been used to create multimaterial devices, including a bionic ear[11] and reactionware for chemical synthesis and analysis.[12] Similarly, nonflowable two-component PDMS elastomers have been used to directly 3D print fluidic chambers[13,14] and synthetic spider webs.[15] It is also possible to alter the viscosity of PDMS prepolymer by incorporating filler materials such as wax microparticles, which can further impart a thermoresponsive behavior to the 3D printed part once cured.[16] In these approaches, the thixotropic behavior of the PDMS prepolymer maintains geometric fidelity during curing. However, the low elastic modulus of the pre- and postcured PDMS and its deformation under gravity still restricts the 3D geometries that can be fabricated, primarily limiting the systems to self-supporting monolithic structures. Thus, some type of support material is

Special Issue: 3D Bioprinting

Received: March 29, 2016
Accepted: May 4, 2016
Published: May 4, 2016

 © 2016 American Chemical Society

DOI: 10.1021/acsbiomaterials.6b00170
ACS Biomater. Sci. Eng. 2016, 2, 1781−1786

required to print more complex 3D PDMS structures. For example, it is possible to print a support material that holds the PDMS prepolymer in place until it can be cured by UV light using a photoactive cross-linking agent developed by the company Wacker Chemie AG.[17] However, it remains to be seen how adaptable this approach is and the resolution and fidelity that can be achieved. Recently, it was demonstrated that soft materials can be 3D printed within microparticulate support baths that behave as a Bingham plastic during the print process.[18,19] Our group showed that a gelatin microparticulate slurry could be used to 3D print soft hydrogels in complex 3D geometries based on biological imaging data, using a process termed freeform reversible embedding of suspended hydrogels (FRESH).[18] Using a similar approach, Bhattacharjee et al. printed hydrogels within a poly(acrylic acid) microparticulate support bath (Carbopol) and PDMS within an oil-based granular gel, achieving high resolution and high fidelity.[19] On the basis of these works, we hypothesized that a hydrophilic, microparticulate support bath could support the embedded printing of PDMS, leveraging the hydrophobic/hydrophilic mismatch, or immiscibility, of the PDMS in water as an additional factor aiding the support of the material during gelation.

Here we report development of a method to 3D print PDMS elastomer in a hydrophilic support bath, designed to enable true freeform fabrication of complex structures. Termed freeform reversible embedding (FRE), FRE printing provides a framework for additive manufacturing of a range of soft polymeric materials. This work is based on previous results using gelatin and Carbopol-based microparticulate supports, but seeks to achieve a number of additional advances important to improving PDMS 3D printing. First, we have exclusively used Sylgard 184 PDMS (Dow Corning), which is the de facto standard in the microfluidics and tissue engineering fields and thus the most relevant for translating 3D PDMS printing to these research areas. Second, we have investigated a range of Carbopol formulations to determine how changes in chemistry and molecular weight impact surface structure of PDMS filaments extruded within these materials. Third, we have varied the temperature during curing of the Sylgard 184 to evaluate how long the material can remain in a pregelled state in the Carbopol without losing dimensional stability. Fourth, we have used changes in salt concentration to modulate the yield stress of the Carbopol to aid removal of delicate PDMS prints from the support bath. Finally, we have 3D printed a range of PDMS structures, focusing on fluidic tubular networks as proof-of-concept for the technology. In total, the results demonstrate the versatility of the FRE printing approach for 3D PDMS fabrication, and should be adaptable to a range of other PDMS types and material systems.

MATERIALS AND METHODS

Preparation of PDMS Ink and Carbopol Support Bath. The PDMS ink for printing was prepared by mixing Sylgard 184 (Dow Corning) in 10:1 base to curing agent ratio and combining and degassing in a planetary centrifugal mixer (Thinky). Optionally, 1−10 drops of black ink from a laboratory marker were added to the PDMS prior to mixing to aid in visualization during printing. The Carbopol support baths were prepared based on manufacturers directions from Carbopol 940, ETD 2020, and Ultrez 30 (Lubrizol). Briefly, 0.1 mL of 10 M NaOH was added to 100 mL of 1.2% w/v Carbopol 940. 0.8 mL of 10 M NaOH was added to 100 mL of 0.7% w/v ETD 2020, and 1 mL of 10 M NaOH was added to 100 mL of 1.0% w/v Ultrez 30 to neutralize the Carbopol gels. Carbopols were mixed and degassed in a planetary centrifugal mixer (Thinky) and then loaded into a container large enough to hold the structure to be 3D printed. For rheological analysis, each Carbopol gel with and without 10× phosphate buffered saline (PBS) added was loaded onto a Gemini 200 Rheometer with a 40 mm, 4° cone (Malvern) and analyzed in frequency sweep from 0.001 to 100 Hz at 150 μm separation and 25 °C.

FRE Printing Process. 3D printing was performed using a Replicator 2 3D printer (MakerBot) with the thermoplastic extruder removed and replaced with a custom designed syringe pump extruder, as previously described.[18] The syringe extruder used the same stepper motor as the thermoplastic extruder, and thus required no software modifications, aside from settings corresponding to nozzle diameter, filament diameter, and "start/end" G-code. The 3D models for printing were designed using SolidWorks CAD software (Dassault Systèmes). All STL files were processed by Slic3r (http://slic3r.org/) software and sliced into 200 μm thick layers to generate G-code instructions for the 3D printer. The helical print G-code was created using the spiral option in the Slic3r software. The G-code was sent to the printer using Pronterface (http://www.pronterface.com/), an open source 3D printer host software suite. Before 3D printing, PDMS ink was drawn into a 10 mL plastic syringe, which was then capped with a 400 μm-ID 0.75″ stainless steel deposition tip (Nordson EFD). The syringe was then mounted into the syringe pump extruder on the 3D printer. A container large enough to hold the structure to be 3D printed was filled with the Carbopol support bath and manually secured to the build platform. The extruder nozzle was positioned at the bottom center of

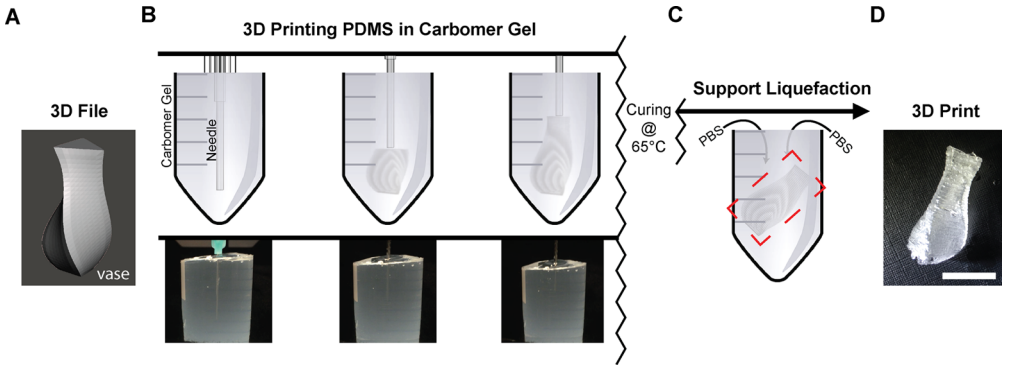

Figure 1. FRE printing is performed by extruding PDMS prepolymer in a support bath consisting of Carbopol gel. (A) A 3D file of a vase is imported and processed into G-code before being 3D printed. (B) The 3D file is replicated, layer-by-layer, from PDMS embedded within the Carbopol support bath by a syringe-based 3D printer. (top) A schematic of the printing process showing the vase in (A) printed within a 50 mL centrifuge tube filled with Carbopol. (bottom) A photograph of the actual vase being 3D printed from PDMS in the Carbopol, due to similar index of refraction it is difficult to see the vase. After printing the PDMS is cured for 72 h at room temperature or 2 h at 65 °C. (C) Following curing of the embedded PDMS, the Carbopol bath is liquefied by addition of monovalent cations, in this case a PBS solution, combined with mechanical agitation. (D) After the support bath is liquefied, the print can be removed. Scale bar is 1 cm.

DOI: 10.1021/acsbiomaterials.6b00170
ACS Biomater. Sci. Eng. 2016, 2, 1781−1786

the support bath, and the print instructions (G-code) were sent to the printer using the host software. Printing took 1 min to 4 h depending on the size and complexity of the printed construct, a typical speed of 20 mm/s. The PDMS was cured while still embedded, either for 72 h at room temperature or for 4 h in an oven at 65 °C. After curing, the prints were released from the support by immersing the printing container in a larger beaker filled with 10X PBS under stirring. After the support bath had liquefied and thinned sufficiently, the prints were gently removed. Hollow prints required extra, manual flushing with 1× PBS solution to remove Carbopol in the luminal space.

Analysis of FRE Printed PDMS Structures. Linear PDMS filaments were FRE printed with diameters 140, 280, and 400 μm in neutralized Carbopol 940, ETD 2020, and Ultrez 30 support baths and cured for 4 h at 65 °C or 72 h at 20 °C. Post curing, the embedded PDMS filaments were removed from the Carbopol and imaged under phase contrast at 10X on a inverted microscope (Nikon). Diameters of the PDMS filaments were measured ten times for each group using ImageJ (National Institutes of Health) and the diameter as a function or cure temperature was statistically analyzed by a *t* test using SigmaPlot 11 (Systat Software, Inc.). To image the 3D surface of the PDMS filaments, we diluted 1 drop of red laboratory marker ink (VWR) in 10 mL of the ink-acetone solution. The PDMS filaments were dipped into acetone for 2 s and then washed in distilled water to stain the surface of the PDMS. Filaments were then imaged under a 555 nm laser on a Zeiss LSM 700 confocal microscope with a 10X objective (NA = 0.3). 3D image stacks were deconvolved with AutoQuant X3 and processed with Imaris 8.2 image analysis software (BitPlane Inc.). To image the 3D surface of the PDMS tube, the same procedure was used accept a tile scan was performed in order to image a larger surface area.

Perfusion of FRE Printed PDMS Tubes. To visualize fluid flow through the FRE printed PDMS tubes, we diluted black food coloring in distilled water and injected into the tubes using a small syringe. Perfusion was carried out on a Nikon SMZ1500 stereomicroscope at 1× magnification and recorded using a Nikon D5100 DSLR camera.

Mechanical Characterization. Uniaxial tensile testing of 3D printed and cast PDMS test samples was performed according to previously described methods.[6] Briefly, PDMS sheets were FRE printed in a vertical configuration with a 0.1 mm layer height and cured in a 67 °C oven for 8 h. These sheets were cut vertically down their face with a razor blade, perpendicular to the layers, to produce rectangular samples approximately 15 mm long, 3.75 mm wide, and 1.75 mm thick. Cast PDMS sheets were cut into samples (dog bones) with a gauge length approximately 25 mm long, 3.45 mm wide and 0.5 mm thick, with additional grip areas 10 mm ling and 7 mm wide. The width and thickness of each individual cast and 3D printed sample was measured before mechanical testing. Uniaxial tensile testing (N = 8 for 3D printed; N = 4 for cast) was performed on an Instron 5943 (Instron) at a strain rate of 2 mm/min until failure. The elastic modulus of each sample was calculated from the slope of the linear region of the stress−strain curves from 0 to 10% strain.

RESULTS AND DISCUSSION

FRE Printing of PDMS in a Hydrophilic Carbopol Support. The FRE printing process works by extruding a hydrophobic PDMS prepolymer within a hydrophilic Carbopol support bath. First, a 3D digital model is created and exported as an STL file (Figure 1A), and then processed into G-code and sent to the 3D printer. Next, the 3D printer is used to extrude the PDMS within the Carbopol, embedding the prepolymer within the support and holding it in place until cured (Figure 1B and Movie S1). After curing, the PDMS is released from the Carbopol by using PBS to shrink the Carbopol microgels and thus decrease the yield stress of the support, effectively fluidizing it when under mild mechanical agitation from a surrounding fluid bath on a magnet stir plate (Figure 1C and Movie S2). Once the PDMS structure is released, it can be removed from the Carbopol, rinsed with distilled water to remove residual Carbopol, and then dried (Figure 1D).

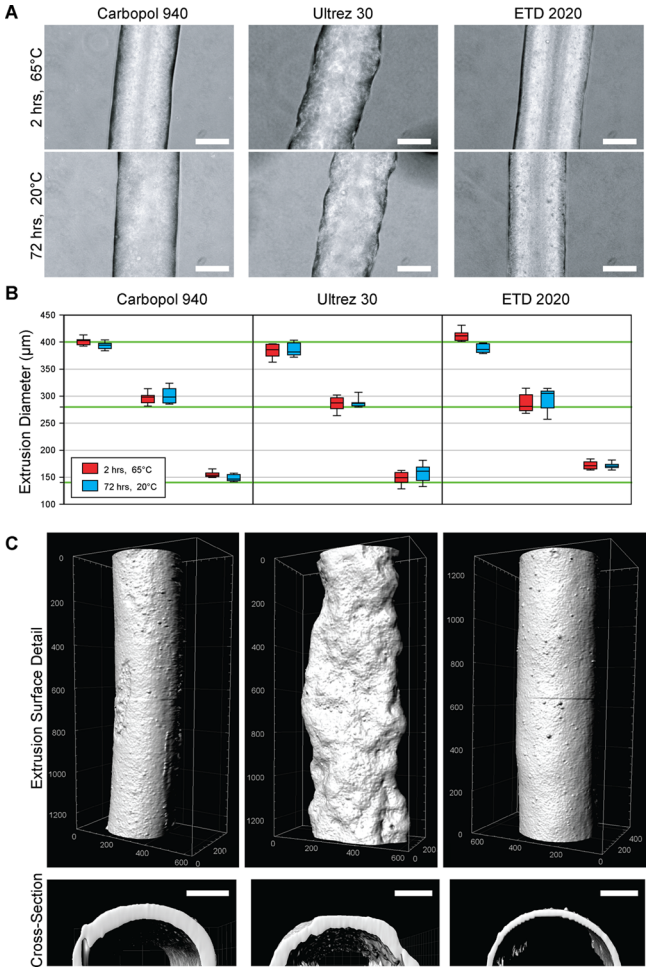

Figure 2. PDMS prepolymer filaments extruder and cured at different temperatures and in different Carbopols are dimensionally stable. (A) Representative phase-contrast images of PDMS filaments extruded into Carbopol 940, ETD 2020 and Ultrez 30 and cured at 65 °C for 2 h or 20 °C for 72 h showed small morphological differences due to the type of Carbopol, but not due to cure temperature (scale bar is 200 μm). (B) Quantification of PDMS filament diameter for target extrusion diameters of 140, 280, and 400 μm (green lines) showed the ability to generally achieve diameters within 10%. The cure temperatures of 65 °C for 2 h (red) and 20 °C for 72 h (blue) did not have a statistically significant effect on diameter (as determined by *t* tests between cure temperatures for each target diameter and Carbopol type, $P < 0.05$). (C) Surface and cross-sectional renderings of PDMS filaments imaged using laser scanning confocal microscopy verified the smooth surface and circular cross-section of PDMS extruded in Carbopol 940 ETD 2020 and the rough surface of PDMS extruded in Ultrez 30 (units in 3D rendering are in micrometers, scale bar is 100 μm).

Dimensional Stability of PDMS Extrusions Cured within the Carbopol Support. The Carbopol must be stable over long periods of time in order to support the PDMS during curing. To test this, we evaluated the effect of both cure temperature and the chemistry and molecular weight of the surrounding Carbopol support on print fidelity. Specifically, we FRE printed PDMS filaments with target diameters of 140, 280, and 400 μm in Carbopol 940, ETD 2020 and Ultrez 30 and cured them either at 65 °C for 2 h or 20 °C for 72 h. Analysis of the PDMS filaments using phase contrast microscopy showed that the Carbopol 940 and ETD 2020 produced smooth, cylindrical filaments while the Ultrez 30 produced

DOI: 10.1021/acsbiomaterials.6b00170
ACS Biomater. Sci. Eng. 2016, 2, 1781−1786

filaments with a rough surface (Figure 2A). There was no apparent difference between the cure temperatures in terms of filament morphology. Quantifying the diameters showed the PDMS filaments were generally within 10% of the target diameter, and confirmed that there was no statistically significant difference in diameter between the cure temperatures (Figure 2B). More detailed 3D analysis of the filament morphology using confocal imaging of fluorescently stained filaments confirmed the smooth surface morphology of the PDMS cured in the Carbopol 940 and ETD 2020 and the rough surface morphology in the Ultrez 30 (Figure 2C). Digitally reconstructed transverse sections from the confocal imaging data confirmed the circular cross-section of the PDMS filaments, expected from the printing of hydrophobic PDMS within a hydrophilic support (Figure 2D).

Releasing FRE Printed PDMS from the Carbopol Support. After the PDMS print is cured inside the Carbopol gel, it is released by liquefying the Carbopol in the presence of ionic solutions. Monovalent cationic buffer solution causes the Carbopol microgels to shrink and lose their bulk plastic behavior. Rheological validation of this effect was shown by comparing the viscosities of Carbopol gels with and without PBS dilutions (Figure 3A). For dilution, 1 mL of diluent was added to 5 mL of Carbopol gel. As a control for the effect of dilution, Carbopol gels that were diluted with deionized water were shown to have a much higher viscosity than those diluted with saline solutions. These results confirm that the Carbopol support is less viscous in the presence of salts, as reported by the manufacturer,[20] and it is this thinning effect that can be leveraged to release prints. To induce thinning of the Carbopol, we submerged embedded PDMS and surrounding support material in PBS solutions under constant stirring (Figure 3B). Over approximately 15 min, it was shown that the Carbopol support would liquefy and release PDMS prints to the surrounding ionic buffer, where they could be retrieved (Figure 3C and Movie S2).

FRE Printing 3D PDMS Structures. Having demonstrated the ability to 3D print PDMS filaments with circular cross-section at the target diameters (Figure 2B) and release the PDMS from the Carbopol support (Figure 3B), we next FRE printed a range of 3D structures to demonstrate the versatility of the process. Carbopol 940 was chosen as the support bath for PDMS prints because large volumes of it required less time to prepare than Ultrez 30 and ETD 2020. Repeating these prints with other Carbopols would likely produce similar results, because extrusion accuracy is consistent regardless of which Carbopol gel was used as a support bath (Figure 2B). As an extension of the previously printed filaments, and to show that FRE printing is truly freeform, we extruded a continuous filament helix with a 1 cm diameter in the Carbopol (Figure 4A, B). This structure is not generated layer-by-layer, and instead as continuous extrusion with the print head moving simultaneously in the X, Y, and Z axes. Equivalent to the linear filaments (Figure 2), the PDMS is well embedded in the Carbopol without collapsing or deforming under gravity. Because the PDMS was allowed to cure while in this shape, the final PDMS object, once released from the Carbopol, retained its initial print geometry (Figure 4C), though the helix was easily deformed once released because of the flexibility of the PDMS.

Next, we demonstrated layer-by-layer FRE printing, showing that layers of Sylgard 184 could be fused together to create mechanically robust structures. We designed a cylindrical shell 2 cm tall and 1.2 cm in diameter (Figure 4D) and FRE printed this within the Carbopol support (Figure 4E). After curing and release from the Carbopol, the cylindrical tube had good fusion between layers; however, at the top of the print approximately the last layer was poorly adhered to the layers below (Figure 4F). This was a consistent phenomenon that was observed, and suggested that layer-to-layer fusion and adhesion of the PDMS required pressure from the layer being extruded above. However, confocal imaging of the surface of a FRE printed tube confirmed that the layers were well fused together (Figure S1), although there were clearly variations in the surface structure where distinct layers could be resolved. As a more challenging test, we designed a 3D helical tube that would be difficult or impossible to create using other PDMS 3D printing approaches (Figure 4G) and printed the PDMS and cured it within the Carbopol support gel (Figure 4H). Though delicate, this helical tube was readily removed from the Carbopol support using PBS to liquefy the Carbopol gel, and the PDMS print retained the intended geometry when suspended in water (Figure 4I). To confirm layer-to-layer fusion, we FRE printed a long PDMS tube (Figure 4J) and perfused it with dye (Figure 4K and Movie S3) and did not observe any leaking. Additionally, we FRE printed sheets of PDMS in a vertical configuration (Figure S2A) and performed uniaxial mechanical testing to show that the elastic modulus was similar to that of cast PDMS controls (Figure S2A, B). It should be noted that although the elastic modulus of the FRE printed

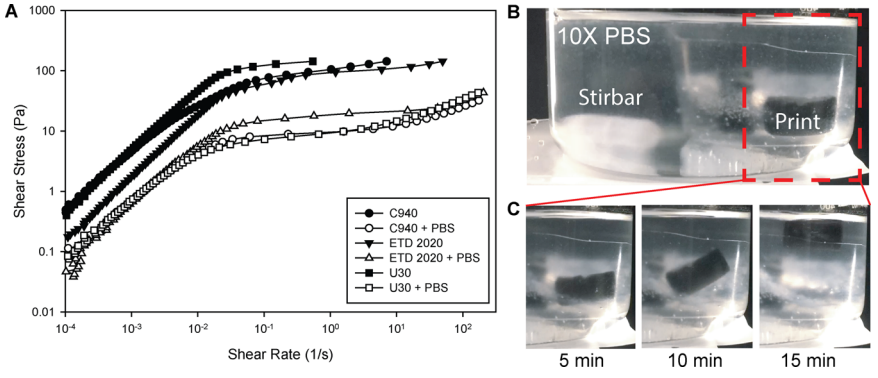

Figure 3. Release of cured PDMS prints by using NaCl solution to decrease yield stress and viscosity. (A) Rheometry of Carbopol gels diluted in water and in PBS buffer demonstrated a thinning behavior in the presence of ionic buffer solutions, whereby they transition from a yield-stress fluid to a shear-thinning fluid. (B) An example of a FRE printed PDMS cylinder (dyed black) in the Carbopol support submerged in a larger beaker consisting of PBS and a magnetically driven stir bar for mechanical agitation. (C) A time-lapse showing the print being released from the Carbopol support by taking advantage of this thinning behavior. Apparent image blurriness is an effect of the Carbopol suspension.

DOI: 10.1021/acsbiomaterials.6b00170
ACS Biomater. Sci. Eng. 2016, 2, 1781−1786

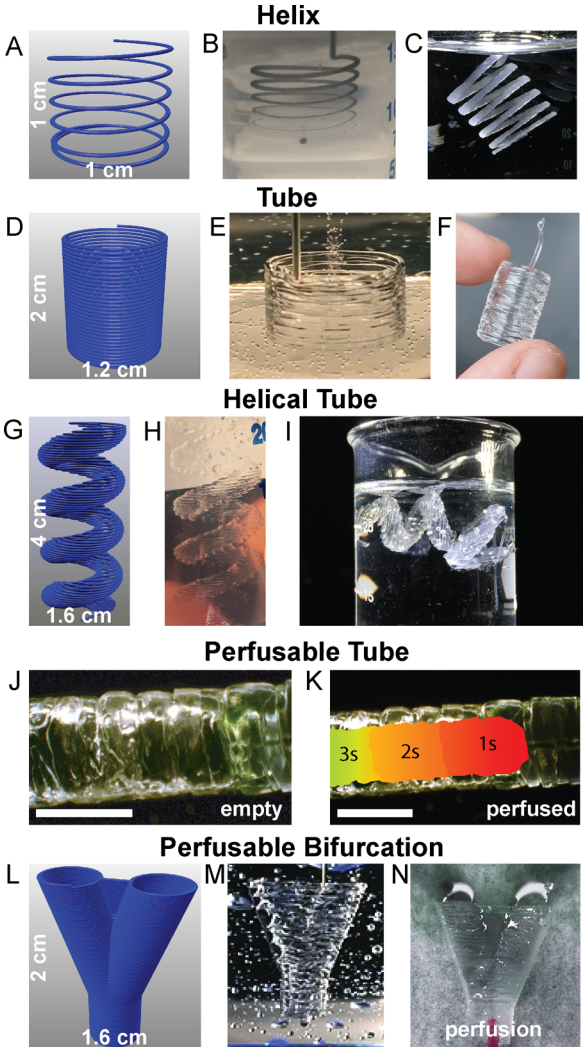

Figure 4. Representative FRE printed PDMS structures using the Carbopol support. (A) The Carbopol gel is capable of supporting freeform extrusion such as this helical path rendered in G-code. (B) The helical extrusion appears identical to the G-code when embedded in the Carbopol (dyed black for visualization). (C) After curing and release, the PDMS helix print retains its geometry when floating in water. (D) G-code for a cylindrical tube created using a helical extrusion. (E) The layers of PDMS filaments fuse into a monolithic surface. (F) After curing and release, the printed tube remains fused between layers and is stiff enough to maintain its geometry while being handled. (G) The G-code for more complex helical tube. (H) As with the tube, the layers of the helical tube are supported within the Carbopol. (I) Release of the helical tube from the Carbopol gel shows the maintenance of geometrical features, supported in water because it cannot support its own weight, even when cured. (J) A PDMS tube to demonstrate the manifold nature of the print's outer surfaces (scale bar is 4 mm). (K) A time-lapse heat map of dye perfused through the tube (scale bar is 4 mm.) (L) G-code of a bifurcation with a webbed fork for stability. (M) The FRE printed PDMS bifurcation embedded in the Carbopol. (N) Perfusion of dye through the bifurcation, splitting fluid flow.

PDMS was found to be less than the cast controls, we believe this was due to underestimating the cross-sectional area because the variability in surface structure (as seen in Figure S1) made it challenging to measure thickness accurately with calipers. Finally, toward potential future applications in FRE printing of 3D PDMS fluidic networks, we designed a bifurcated tube (Figure 4L) and then printed and cured it in the Carbopol support (Figure 4M). The bifurcated tube was then perfused and shown to be manifold and capable of splitting fluid flow (Figure 4N and Movie S4). In total, these results show that FRE printing can be used to create 3D PDMS structures in both continuous freeform extrusion and layer-by-layer approaches. By using Sylgard 184, we demonstrate that precured prints are stable for long periods of time prior to gelation and that complex 3D architectures are well maintained in the Carbopol support.

While FRE printing can be used to create complex 3D PDMS structures using Carbopol as an immiscible support material, there are limitations. We found that the process works well for extruded filaments where the immiscibility of the PDMS in the aqueous Carbopol produces a consistent circular cross-section due to surface energy minimization (Figure 2). The aberrant morphology of PDMS in Ultrez 30 is poorly understood and requires further investigation, but may be due to larger microgel size. The FRE process also works well for 3D structures printed as solid shells, as demonstrated for the various PDMS tubes (Figure 4). However, the FRE process of printing PDMS in Carbopol as currently described in this manuscript does not work well for the lateral fusion of extruded PDMS filaments. In other words, as shown for the cylindrical tube (Figure 4F), it appears that the pressure applied from the deposition of additional layers is required to aid fusion of layers below. This pressure is absent when filaments are extruded next to each other in the same XY plane, and thus we were unable to achieve lateral fusion with the current setup (data not shown). Overcoming this lateral fusion limitation will need to be an area of future research in order to achieve 3D PDMS prints where standard infill algorithms can be used to build internal structure of 3D parts. Additionally, the use of the Carbopol support means that the material can become trapped within void spaces inside the print. This can be addressed in a manner similar to that used for selective laser sintering and stereolithography, specifically by providing small holes that can be used for support/material removal after printing.

CONCLUSION

Here we have demonstrated a new method of 3D printing PDMS using a hydrophilic Carbopol support. FRE printing enables the 3D assembly and confinement of slowly curing materials by placing them into a fugitive, plastic support that they cannot diffuse into during gelation due to immiscibility. While this process works for PDMS, there are also other hydrophobic polymer resins such as cycloaliphatic epoxies and fluoroelastomers that may also be adaptable to FRE printing using Carbopol. Thus, we envision this methodology will be applicable to a wide range of materials. As noted, there are current limitations with the approach, primarily the lateral fusion between extruded PDMS filaments. However, as we gain a better understanding of the FRE printing process we anticipate this will be overcome by changing support bath and/or PDMS ink chemistry or by modifying machine printing parameters. Specifically, changing the viscosity of the PDMS ink so that it is thixotropic should maintain the printing capability while reducing flow after extrusion, which should reduce the variability in fusion. The open-source nature of the FRE printing platform should also accelerate this development process, because it enables easy adoption of the technology using widely accessible and low cost 3D printers.

DOI: 10.1021/acsbiomaterials.6b00170
ACS Biomater. Sci. Eng. 2016, 2, 1781−1786

■ ASSOCIATED CONTENT

Supporting Information

The Supporting Information is available free of charge on the ACS Publications website at DOI: 10.1021/acsbiomaterials.6b00170.

Uniaxial tensile testing of FRE printed PDMS strips, elastic modulus of FRE printed versus cast PDMS sample, and 3D confocal imaging of the surface of a FRE printed PDMS tube (PDF)

Movie S1, FRE printing of PDMS in the Carbopol support (MPG)

Movie S2, Release of the PDMS structure from the Carbopol support (MPG)

Movie S3, Liquid perfusion through a FRE printed PDMS tube (MPG)

Movie S4, Liquid perfusion through a FRE printed PDMS bifurcated tube (MPG)

■ AUTHOR INFORMATION

Corresponding Author

*E-mail: feinberg@andrew.cmu.edu.

Notes

The authors declare the following competing financial interest(s): Carnegie Mellon University has filed for patent protection on the technology described herein, and T.J.H. and A.W.F.are named as inventors on the patent..

■ ACKNOWLEDGMENTS

We thank Dr. Rachelle Palchesko Simko for technical assistance with uniaxial tensile testing. This work was supported by the National Institutes of Health Director's New Innovator Award (DP2HL117750), Disruptive Health Technology Institute, Carnegie Mellon University (A017261-HIGHMARK-Feinberg) and the National Science Foundation CAREER Award (1454248).

■ REFERENCES

(1) Belanger, M. C.; Marois, Y. Hemocompatibility, biocompatibility, inflammatory and in vivo studies of primary reference materials low-density polyethylene and polydimethylsiloxane: a review. *J. Biomed. Mater. Res.* **2001**, *58* (5), 467−77.

(2) Piruska, A.; Nikcevic, I.; Lee, S. H.; Ahn, C.; Heineman, W. R.; Limbach, P. A.; Seliskar, C. J. The autofluorescence of plastic materials and chips measured under laser irradiation. *Lab Chip* **2005**, *5* (12), 1348−54.

(3) Hua, F.; Sun, Y.; Gaur, A.; Meitl, M. A.; Bilhaut, L.; Rotkina, L.; Wang, J.; Geil, P.; Shim, M.; Rogers, J. A.; Shim, A. Polymer Imprint Lithography with Molecular-Scale Resolution. *Nano Lett.* **2004**, *4* (12), 2467−71.

(4) Charati, S. G.; Stern, S. A. Diffusion of Gases in Silicone Polymers: Molecular Dynamics Simulations. *Macromolecules* **1998**, *31* (16), 5529−35.

(5) Whitesides, G. M.; McDonald, J. C. Poly (dimethylsiloxane) as a Material for Fabricating Microfluidic Devices. *Acc. Chem. Res.* **2002**, *35*, 491−499.

(6) Comina, G.; Suska, A.; Filippini, D. PDMS lab-on-a-chip fabrication using 3D printed templates. *Lab Chip* **2014**, *14* (2), 424−30.

(7) Palchesko, R. N.; Zhang, L.; Sun, Y.; Feinberg, A. W. Development of Polydimethylsiloxane Substrates with Tunable Elastic Modulus to Study Cell Mechanobiology in Muscle and Nerve. *PLoS One* **2012**, *7*, e51499.

(8) Sun, Y.; Jallerat, Q.; Szymanski, J. M.; Feinberg, A. W. Conformal nanopatterning of extracellular matrix proteins onto topographically complex surfaces. *Nat. Methods* **2015**, *12* (2), 134−136.

(9) Kim, D.-H.; Ghaffari, R.; Lu, N.; Rogers, J. A. Flexible and Stretchable Electronics for Biointegrated Devices. *Annu. Rev. Biomed. Eng.* **2012**, *14* (1), 113−28.

(10) Ratner, B. D.; Hoffman, A. S.; Schoen, F. J.; Lemons, J. E. *Biomaterials Science: An Introduction to Materials in Medicine*, 3rd ed.; Academic Press: Cambridge, MA, 2013; p 1573.

(11) Mannoor, M. S.; Jiang, Z.; James, T.; Kong, Y. L.; Malatesta, K. a.; Soboyejo, W. O.; Verma, N.; Gracias, D. H.; McAlpine, M. C. 3D printed bionic ears. *Nano Lett.* **2013**, *13*, 2634−9.

(12) Symes, M. D.; Kitson, P. J.; Yan, J.; Richmond, C. J.; Cooper, G. J. T.; Bowman, R. W.; Vilbrandt, T.; Cronin, L. Integrated 3D-printed reactionware for chemical synthesis and analysis. *Nat. Chem.* **2012**, *4* (5), 349−54.

(13) Kolesky, D. B.; Truby, R. L.; Gladman, A. S.; Busbee, T. A.; Homan, K. A.; Lewis, J. A. 3D Bioprinting of Vascularized, Heterogeneous Cell-Laden Tissue Constructs. *Adv. Mater.* **2014**, *26* (19), 3124−3130.

(14) Kolesky, D. B.; Homan, K. A.; Skylar-Scott, M. A.; Lewis, J. A. Three-dimensional bioprinting of thick vascularized tissues. *Proc. Natl. Acad. Sci. U. S. A.* **2016**, *113* (12), 3179−84.

(15) Qin, Z.; Compton, B. G.; Lewis, J. A.; Buehler, M. J., Structural optimization of 3D-printed synthetic spider webs for high strength. *Nat. Commun.* **2015**, *6*.7038703810.1038/ncomms8038

(16) Lipton, J. I.; Angle, S.; Lipson, H. 3D Printable Wax-Silicone Actuators. In *2014 Annual International Solid Freeform Fabrication Symposium*; Austin, TX, Aug 4−6, 2014 ; Laboratory for Freeform Fabrication and University of Texas: Austin, TX, 2014; pp 848−56.

(17) *Interim Report January − June 2015:3D Printing with Silicones*; Wacker Chemie AG: August 3, 2015, 2015; pp 5−10.

(18) Hinton, T. J.; Jallerat, Q.; Palchesko, R. N.; Park, J. H.; Grodzicki, M. S.; Shue, H.-J.; Ramadan, M. H.; Hudson, A. R.; Feinberg, A. W. Three-dimensional printing of complex biological structures by freeform reversible embedding of suspended hydrogels. *Science Advances* **2015**, *1* (9), e1500758.

(19) Bhattacharjee, T.; Zehnder, S.; Rowe, K.; Jain, S.; Nixon, R.; Sawyer, G.; Angelini, T. Writing in the Granular Gel Medium. *Science Advances* **2015**, *1* (8), e1500655.

(20) *Technical Data Sheet 730: Viscosity of Carbopol* Polymers in Aqueous Systems*; Lubrizol Advanced Materials: Wickliffe, OH, 2010; pp 1−10.

DOI: 10.1021/acsbiomaterials.6b00170
ACS Biomater. Sci. Eng. 2016, 2, 1781−1786